




Molar masses and molar mass distributions of commercial regenerated cellulose materials and softwood dissolving pulp determined by SEC/MALLS

Yuko Ono · Gaoyuan Hou · Korawit Chitbanyong ·
Miyuki Takeuchi · Akira Isogai 

Received: 9 May 2023 / Accepted: 18 July 2023 / Published online: 26 July 2023
© The Author(s) 2023

Abstract The molar masses and molar mass distributions of three commercial regenerated cellulose samples, viscose rayon, Tencel, and Bemliese (or cuprammonium nonwoven), have been determined by dissolution in 8% (w/w) lithium chloride/*N,N*-dimethylacetamide (LiCl/DMAc) and subsequent size-exclusion chromatography with multi-angle laser-light scattering detection (SEC/MALLS). Before dissolution in LiCl/DMAc, the regenerated cellulose samples were pretreated by the following three methods: (1) soaking in ethylene diamine (EDA) and subsequent solvent exchange to *N,N*-dimethylacetamide (DMAc) through methanol, (2) soaking in water and subsequent solvent exchange to DMAc through ethanol, and (3) soaking in water and subsequent solvent exchange to tert-butyl alcohol through ethanol and freeze drying. The pretreated samples were dissolved in 8% (w/w) LiCl/DMAc by stirring the cellulose/LiCl/DMAc mixtures for 1–3 weeks followed by

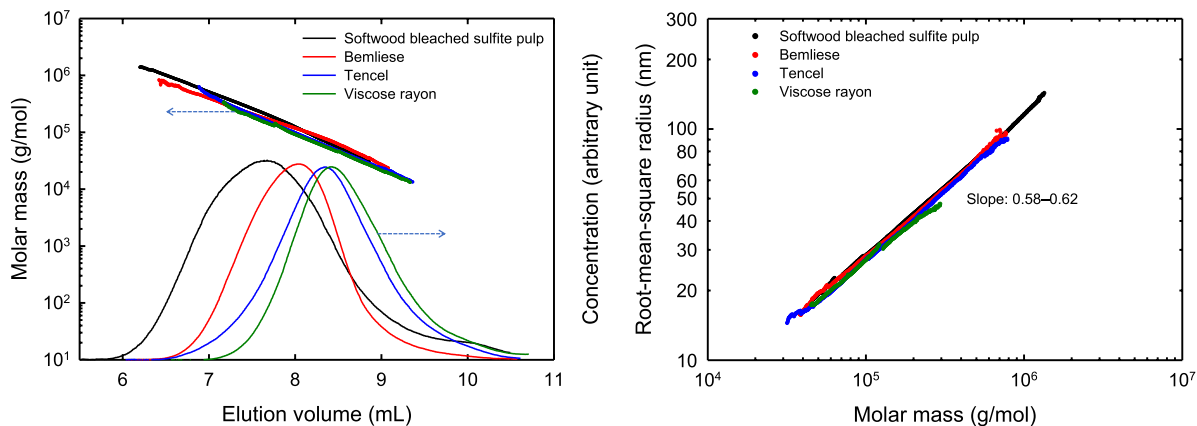
dilution to 1% (w/v) LiCl/DMAc for SEC/MALLS analysis. The EDA- and water-pretreated samples gave almost the same SEC-elution patterns and molar mass plots, resulting in similar number- and mass-average molar masses. However, the freeze-dried samples gave 10%–20% lower mass recovery ratios than those obtained for the EDA- or water-pretreated samples, probably because of incomplete dissolution of the freeze-dried samples in 8% (w/w) LiCl/DMAc. The average mass-average degree of polymerization values of viscose rayon, Tencel, and Bemliese were 340, 530, and 880, respectively. The slopes of the conformation plots were 0.58–0.62, showing that all of the molecules in the three regenerated cellulose samples were dissolved in 1% (w/v) LiCl/DMAc, forming linear random-coil conformations.

Supplementary Information The online version contains supplementary material available at <https://doi.org/10.1007/s10570-023-05414-2>.

Y. Ono · G. Hou · K. Chitbanyong · A. Isogai (✉)
Department of Biomaterials Science, Graduate School
of Agricultural and Life Sciences, The University
of Tokyo, Tokyo 113-8657, Japan
e-mail: akira-isogai@g.ecc.u-tokyo.ac.jp

M. Takeuchi
Institute of Engineering Innovation, The University
of Tokyo, Tokyo 113-8656, Japan

Graphical abstract



Sample	M_n	M_w	DP_w	M_w/M_n	Calculated mass (μg)	Slope of conformation plots
Viscose rayon	26900 ± 1570	54400 ± 1540	340 ± 10	2.0 ± 0.1	48.1 ± 0.6	0.58
Tencel	32700 ± 1120	86600 ± 3280	530 ± 20	2.0 ± 0.2	50.8 ± 3.5	0.59
Bemliese	87600 ± 4350	143100 ± 1060	880 ± 7	1.6 ± 0.1	65.3 ± 1.6	0.59
Softwood bleached sulfite pulp	72200 ± 1770	293100 ± 9180	1810 ± 60	4.1 ± 0.2	51.5 ± 0.9	0.62

Keywords LiCl · DMAc · Molar mass parameters · SEC/MALLS · Solid-state ^{13}C -NMR · Regenerated cellulose material

Introduction

Regenerated cellulose fiber is important for textiles, engineering filament yarns, and various medical and healthcare applications. Viscose rayon, Tencel (or Lyocell), and Bemliese (or cuprammonium non-woven) are typical regenerated cellulose materials produced at the industrial level, and they have contributed to our cultural lives and technologies for a long time (Fink et al. 2001; Sayyed et al. 2019; Veit 2022). Although viscose rayon production and wastewater treatment systems have some environmental issues caused by H_2S emission into the atmosphere, viscose rayon is still the main regenerated cellulose fiber, and it is called artificial silk in man-made fibers (Li et al. 2018; Kuchtoá et al. 2023). Tencel has been

developed to overcome some of the shortcomings of the viscose rayon production process and to improve the fiber quality (Fink et al. 2001; Kreze and Malei 2003; Abu-Rous et al. 2007; Borbély 2008; Sayyed et al. 2019; Veit 2022). Bemliese is another category of regenerated cellulose materials.

Viscose rayon and Tencel are produced by dissolution of wood dissolving pulps with high α -cellulose contents (> 93%) in aqueous CS_2/NaOH at room temperature and thermally melted *N*-methylmorpholine *N*-oxide (NMMO) hydrate, respectively, and subsequent spinning, regeneration in aqueous media, washing with water, and drying. Bemliese is produced from cotton linters cellulose by dissolution in aqueous $\text{Cu}(\text{NH}_3)_4(\text{OH})_2$, spinning, fabrication, regeneration in an aqueous medium, washing with water, and drying to form cuprammonium nonwoven, which is mainly used for medical, healthcare, and agribusiness applications (Veit 2022).

The molar masses and molar mass distributions of these regenerated cellulose materials are

fundamental and important factors that influence the mechanical and other key properties of the materials. Size-exclusion chromatography combined with multi-angle laser-light scattering and refractive index detection (SEC/MALLS/RI) gives molar-mass distributions and number- and mass-average molar mass values (M_n and M_w , respectively). In this case, the cellulose samples should be completely dissolved in a solvent at the individual molecular level, and the solution should be transparent (without fluorescence formed by laser-light irradiation). Furthermore, the cellulose molecules should be stable in the solvent without depolymerization or side reactions during the dissolution process and storage of the cellulose solution. Lithium chloride/*N,N*-dimethylacetamide (LiCl/DMAc) is the only solvent system that satisfies the above requirements (Bikova and Treimanis 2002; Potthast et al. 2003; Dupont 2003; Ono and Isogai 2020). Some activation methods or pretreatments of the cellulose sample are required before dissolution treatment in 8% (w/w) LiCl/DMAc for complete dissolution (Bikova and Treimanis 2002; Potthast et al. 2003; Dupont 2003). However, it has been reported that complete dissolution of regenerated cellulose materials is often difficult, resulting in inaccurate molar mass data by SEC/MALLS (Henninges et al. 2014; Siller et al. 2014; Silbermann et al. 2017).

The water-activation method followed by solvent exchange to DMAc through acetone has been used to pretreat some cellulose samples, such as hardwood bleached kraft pulps, softwood and hardwood bleached sulfite and prehydrolyzed kraft pulps, and cotton linters cellulose samples, for dissolution in 8% (w/w) LiCl/DMAc (Bikova and Treimanis 2002; Potthast et al. 2003; Dupont 2003; Henninges et al. 2014; Siller et al. 2014). However, softwood bleached kraft pulps (SBKPs), cotton lint, bacterial, tunicate, and algal cellulose samples, hemicellulose-rich plant holocellulose samples, and some regenerated cellulose samples cannot be completely dissolved in 8% (w/w) LiCl/DMAc by the water-activation method (Henninges et al. 2014; Siller et al. 2014; Silbermann et al. 2017).

In previous work, we succeeded in completely dissolving all of the above native cellulose and plant holocellulose samples in 8% (w/w) LiCl/DMAc by 100% ethylene diamine (EDA) pretreatment. The

cellulose and holocellulose samples were first soaked in EDA, and EDA was then solvent exchanged to DMAc through methanol. Complete dissolution was achieved by stirring the EDA-pretreated cellulose and holocellulose samples in 8% (w/w) LiCl/DMAc at room temperature for a few days, weeks, or months depending on the sample. The key for complete dissolution of all of the native cellulose and holocellulose samples is conversion of the cellulose I crystal structure in the sample to cellulose III or disordered structures by EDA treatment followed by methanol washing. The cellulose and holocellulose solutions in 8% (w/w) LiCl/DMAc are then diluted to 1% (w/v) LiCl/DMAc and subjected to SEC/MALLS analysis. Consequently, some important information about the native cellulose samples and plant holocelluloses have been obtained by SEC/MALLS (Ono et al. 2016a, b, 2017, 2018, 2021, 2022a, b; c; Ono and Isogai 2020). It is possible that low-molar-mass hemicellulose molecules slightly dissolve in EDA during pretreatment and are excluded from the SEC/MALLS data, which should be taken into account (Yamamoto et al. 2011).

In this study, two regenerated cellulose fibers, viscose rayon and Tencel, and one regenerated nonwoven cellulose, Bemliese, were selected, and the following three pretreatments were applied to the regenerated cellulose samples: EDA soaking used in our previous studies, conventional water soaking, and water-soaking/freeze-drying. In the EDA- and water-soaking pretreatments, some mass losses may be unavoidable during repeated solvent exchange and centrifugation, resulting in inaccurate cellulose concentrations in the obtained LiCl/DMAc solutions used for SEC/MALLS. In contrast, more accurate cellulose concentrations of the LiCl/DMAc solutions are obtained using freeze-dried samples, which is significant for evaluation of complete dissolution in LiCl/DMAc from mass loss values (caused by, for example, incomplete dissolution) in SEC/MALLS analysis. Soaking of cellulose samples including some regenerated cellulose fibers in dimethylsulfoxide followed by solvent-exchange to DMAc has been reported for complete dissolution in LiCl/DMAc for SEC/MALLS analysis (Silbermann et al. 2017). However, the mass recovery ratios of the starting cellulose materials in the LiCl/DMAc solutions subjected to SEC/MALLS analysis were not taken into account, and no data for water-activated or freeze-dried cellulose samples

were provided. In this study, one softwood bleached sulfite pulp (SBSP) sample, which was prepared by acid sulfite pulping and subsequent bleaching and used as the dissolving pulp for production of viscose rayon and some cellulose derivatives, was also applied to dissolution in 8% (w/w) LiCl/DMAc and subsequent SEC/MALLS analysis as a reference (Mendes et al. 2021).

Materials and methods

Samples

The viscose rayon and Tencel fibers were commercial products. Bemliese (or cuprammonium nonwoven) was kindly provided by Asahi Kasei Co., Ltd. (Miyazaki, Japan). The regenerated samples were cut into short lengths of 3–5 mm with scissors. The SBSP was dissolving pulp fibers produced from softwood chips by acid sulfite pulping and subsequent bleaching processes (Nippon Paper Co. Ltd., Japan). This SBSP contained 96% glucose, 1.5% xylose, and 0.9% mannose as neutral sugars (Ono et al. 2018). The 1 M cupriethylenediamine hydroxide solution ($\text{Cu}(\text{EDA})_2(\text{OH})_2$) is a commercial product (Sigma Aldrich, USA). LiCl, DMAc, and the other chemicals and solvents were laboratory grade (FUJIFILM Wako Pure Chemical, Co., Tokyo, Japan) and used as received.

Dissolution of the cellulose samples in 8% (w/w) LiCl/DMAc

The three regenerated cellulose samples (viscose rayon, Tencel, and Bemliese) and SBSP were dissolved in 8% (w/w) LiCl/DMAc according to the procedures shown in Fig. 1. The first procedure was followed by the EDA-activation method commonly used in our laboratory (Ono et al. 2016a, b, 2020). After vacuum drying at 40 °C for 1 day, the cellulose sample (20 mg on dry mass) was soaked in 100% EDA (5 mL), and the mixture was stirred with a magnetic stir bar overnight. Solvent exchange from EDA to methanol (MeOH, 35 mL) was then performed by centrifugation, and the cellulose/MeOH mixture was shaken overnight. This treatment was repeated twice with fresh MeOH (35 mL each). The mixture was then solvent exchanged from MeOH to

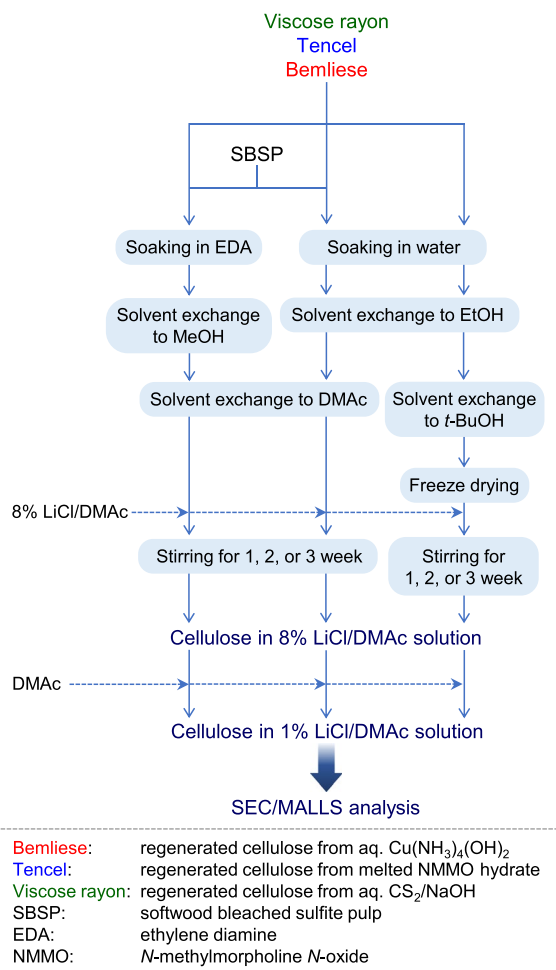


Fig. 1 Scheme for dissolution of the three regenerated cellulose samples and one dissolving pulp in 8% (w/w) LiCl/DMAc by three activation methods for SEC/MALLS analysis of the cellulose samples

DMAc (35 mL) by centrifugation and shaking the cellulose/DMAc mixture overnight. This treatment was repeated again with fresh DMAc. After centrifugation of the mixture to remove excess DMAc, 8% (w/w) LiCl/DMAc (5 g) was added to the cellulose sample, and the mixture was stirred at ~23 °C for 1 or 2 weeks.

The second procedure was followed by the conventional water-activation method (Bikova and Treimanis 2002; Dupont 2003; Henninges et al. 2014) with slight modification. The vacuum-dried sample (20 mg on dry mass) was soaked in water (20 mL), and the mixture was stirred overnight. Solvent exchange from water to ethanol (EtOH, 35 mL) was then performed

by centrifugation, and the mixture was shaken overnight. This treatment was repeated twice with fresh EtOH (35 mL each). Solvent exchange from EtOH to DMAc was then performed by centrifugation, and the cellulose/DMAc mixture was stirred overnight. This treatment was repeated again with fresh DMAc. After centrifugation of the mixture to remove excess DMAc, 8% (w/w) LiCl/DMAc (5 g) was added to the cellulose sample, and the mixture was stirred at ~ 23 °C for 1, 2, or 3 weeks.

In the third procedure, the three regenerated cellulose samples were dissolved in 8% (w/w) LiCl/DMAc according to the following freeze-drying method. The vacuum-dried sample (50 mg on dry weight) was soaked in water (20 mL), and the mixture was stirred overnight. Solvent exchange from water to EtOH (35 mL) was then performed, and the mixture was shaken for 3 h. Solvent exchange from EtOH to *tert*-butyl alcohol (*t*-BuOH) was then performed, and the mixture was shaken for 3 h. This treatment was repeated again with fresh *t*-BuOH followed by freeze drying for 5 days. The freeze-dried sample (8 mg) was dispersed in 8% (w/w) LiCl/DMAc (2 g), and the mixture was stirred at ~ 23 °C for 1, 2, or 3 weeks.

SEC/MALLS analysis

The cellulose solutions in 8% (w/w) LiCl/DMAc obtained by the processes described in the previous section were diluted with fresh DMAc to prepare cellulose solutions in $\sim 1\%$ (w/v) LiCl/DMAc. Each solution was passed through a 0.45- μm poly(difluoroethylene) disposable filter (Millex, Merck Millipore, Tokyo, Japan) and then subjected to SEC/MALLS analysis with 1% (w/v) LiCl/DMAc as the eluent (Ono et al. 2016b, 2022a, c). KD-806 M and KD-G columns (Shodex, Tokyo, Japan) were used as the SEC and guard columns, respectively. A MALLS detector (DOWN HELEOS-II, $\lambda = 658$ nm; Wyatt Technologies, USA) and a refractive index detector (RID-10A, Shimadzu, Japan) were set in a high-pressure liquid chromatograph system. ASTRA software (version 6.1, Wyatt Technologies, USA) was used for data acquisition and the analyses. The number- and mass-average molar masses (M_n and M_w , respectively) of the cellulose samples were calculated using the value of 0.131 mL/g as the specific refractive index increment (dn/dc) (Ono et al. 2016a).

Viscosity-average degrees of polymerization of the cellulose samples

The freeze-dried cellulose sample (0.04 g) was soaked in water (10 mL), and the mixture was stirred for 10 min. The 1 M $\text{Cu}(\text{EDA})_2(\text{OH})_2$ solution (10 mL) was added to the cellulose/water mixture, and the solution was stirred until the cellulose sample was completely dissolved in 0.5 M $\text{Cu}(\text{EDA})_2(\text{OH})_2$ (20 mL). The viscosity ratio of the solution η_{rel} was measured using a Cannon–Fenske-type capillary viscometer. The limiting viscosity number $[\eta]$ (or intrinsic viscosity) was calculated from the viscosity relative increment η_{sp} (or specific viscosity) using the Schulz–Blaschke equation (Schulz and Dinglinger 1941): $[\eta] = \eta_{\text{sp}}/c(1 + 0.28\eta_{\text{sp}})$, where c is the cellulose concentration (g/mL). The DP_v value of the sample was calculated from $[\eta]$ using the Mark–Houwink–Sakurada equation: $[\eta] = 0.909 \times \text{DP}_v^{0.9}$ (Marx 1955; Isogai et al. 1989a, b).

Solid-state ^{13}C -NMR analysis

Each of the air-dried cellulose samples was set in a ZrO_2 sample rotor, and the solid-state ^{13}C NMR spectrum was obtained by a NMR system (JNM-ECA II 500, JEOL, Tokyo, Japan) equipped with a cross-polarization (CP) and magic-angle sample-spinning probe (Funahashi et al. 2017; Ono et al. 2022a, b, c) under the following conditions: a sample spinning rate of 15 kHz, a proton 90° pulse time of 2.5 μs , and a relaxation delay of 5 s. CP transfer was achieved using a ramped amplitude sequence for a CP contact time of 2 ms. Each spectrum was acquired by 12,000 scans for 16 h.

Results

Solid-state ^{13}C -NMR spectra of the cellulose samples

The solid-state ^{13}C -NMR spectra of the three regenerated cellulose samples and SBSP are shown in Fig. 1. Viscose rayon, Tencel, and Bemliese exhibited typical NMR patterns of low-crystallinity cellulose II samples. The crystalline C1 carbon peaks appeared at 105 and 107 ppm, and the crystalline C4 carbon peaks appeared at 88 and 89 ppm (Horii et al. 1982; Zhao et al. 2007; Östlund et al. 2013; Idström et al.

2016). The C6-OH carbon atoms of the three regenerated cellulose samples exhibited broad single peaks at ~63 ppm, showing that they had gauche–trans and gauche–gauche conformations, which correspond to the C6-OH groups of cellulose II and amorphous structures, respectively (Horii et al. 1983; Larsson PT 2005; Funahashi et al. 2017). The NMR spectrum of SBSP showed the typical pattern of wood chemical pulp (Zhou et al. 2020), and the crystallinity of cellulose I measured from the peak areas of the crystalline and amorphous C4 carbon atoms ($C4_{\text{cry}}$ and $C4_{\text{amo}}$, respectively, in Fig. 2) was 56%. The relative peak areas of C6/C1 for the four samples in Fig. 2 were 0.78–0.83 (Yang et al. 2018; Zhou et al. 2020; Ono et al. 2021, 2022c).

Each of the regenerated cellulose samples had a small peak (C') at ~97 ppm, which is the same as those of the C1 carbon atoms of the reducing ends (Dudley et al. 1983; Isogai et al. 1989a, b; Moulthrop et al. 2005; Yuan et al. 2022). However, the

peak ratios of $(C1 + C')/C1'$ (or the DP_n values calculated from the ^{13}C peak ratios) were 25, 40, and 42 for viscose rayon, Tencel, and Bemliese, respectively, which are not plausible because the DP_n values of the regenerated cellulose samples determined by SEC/MALLS were much higher than 170, as described in the following section. Some solid-state ^{13}C NMR spectra of viscose rayon samples in the literature exhibit the same small peaks at ~97 ppm (Horii et al. 1982; Ibbett et al. 2007; Zhao et al. 2007; Li et al. 2012; Shanshan et al. 2012; Mori et al. 2012; Wei et al. 2018; Zhang et al. 2018; From et al. 2020; Fadavi et al. 2021), whereas other regenerated cellulose samples do not show the corresponding small peaks (Newman and Hemmingson 1994; Ago et al. 2004; Jin et al. 2007; Duchemin et al. 2007; Östlund et al. 2013; Idström et al. 2016). The small peak at ~97 ppm appears in the NMR spectra of some dried regenerated cellulose samples (Nomura et al. 2020), whereas mercerized cellulose does not show such a peak (Maunu et al. 2000).

Some TEMPO-oxidized cellulose samples without post-oxidation with NaClO_2 or post-reduction with NaBH_4 (Shinoda et al. 2012) show the corresponding small peaks at ~97 ppm in their solid-state ^{13}C -NMR spectra (Follain et al. 2010; Biliuta et al. 2010; Cao et al. 2012; Li et al. 2017; Lin et al. 2017). These TEMPO-oxidized cellulose samples contain small amounts of C6-aldehydes formed as intermediates (Isogai et al. 2011, 2018; Isogai 2022). Thus, it is possible that the C' peak at ~97 ppm for the regenerated cellulose samples can be ascribed to hydrated C6-aldehydes, which are formed by partial oxidation of the C6-OH groups during the dissolution, aging, spinning/regeneration, and/or drying process in the commercial production system. The extended ^{13}C -NMR spectra of the cellulose samples are shown in Fig. S1 in the Electronic Supplementary Material. Although the three regenerated cellulose samples exhibited no clear $\text{C}=\text{O}$ peaks owing to carboxy, aldehyde, and/or ketone groups in the region 170–235 ppm, the intensity-magnitude spectra indicated the presence of small $\text{C}=\text{O}$ peaks at 197–198 ppm. The presence of $\text{C}=\text{O}$ groups in regenerated cellulose samples has been reported by Potthast et al. (2003).

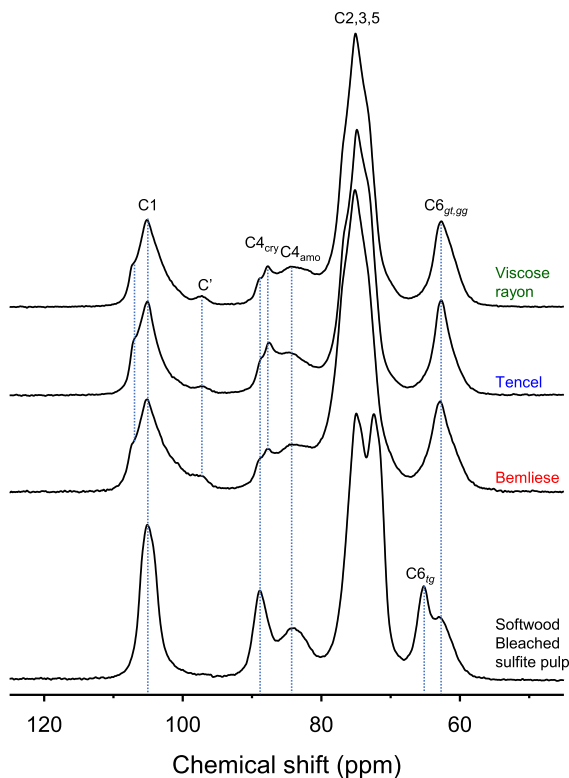


Fig. 2 Solid-state ^{13}C -NMR spectra of the three regenerated cellulose samples (viscose rayon, Tencel, and Bemliese) and dissolving pulp (SBSP)

SEC/MALLS analysis of the regenerated cellulose samples and SBSP

The three regenerated cellulose samples were pre-treated by the three methods (EDA soaking, water soaking, and freeze drying) (Fig. 1), and the pre-treated samples were stirred in 8% (w/w) LiCl/DMAc for 1–3 weeks. Freeze-dried wood chemical pulps, such as SBSP, are insoluble in 8% (w/w) LiCl/DMAc, and thus only the EDA- and water-soaking treatments were applied to SBSP before stirring in 8% (w/w) LiCl/DMAc. All of the EDA- and water-pretreated samples visually dissolved in 8% (w/w) LiCl/DMAc within 1 week. The freeze-dried Tencel and Bemliese samples visually dissolved in 8% (w/w) LiCl/DMAc, whereas freeze-dried viscose rayon in 8% (w/w) LiCl/DMAc was slightly cloudy even after stirring the mixture for 2 weeks, probably because of the presence of a

small amount of insoluble particles (Siller et al. 2014).

The SEC/MALLS results of viscose rayon are shown in Fig. 3a, Figs. S2–S4, and Tables S1–S3. The molar mass plots for the three pretreatments agreed well (Fig. 3a). The peak areas of the SEC-elution patterns roughly corresponded to the sample masses injected into the SEC/MALLS system. The SEC-elution peak area of the viscose rayon sample pretreated by freeze drying was smaller than those pretreated by EDA and water soaking (Fig. 3a). The lower calculated mass value of the freeze-dried viscose rayon (42 μg , Table S3) than those of EDA-soaked and water-soaked viscose rayon (48 μg , Tables S1 and S2) indicates some mass loss. This was probably caused by filtration of insoluble particles present in the 8% (w/w) LiCl/DMAc solution. However, the other molar mass parameters, such as M_n , M_w , DP_w , and M_w/M_n , were similar for the three

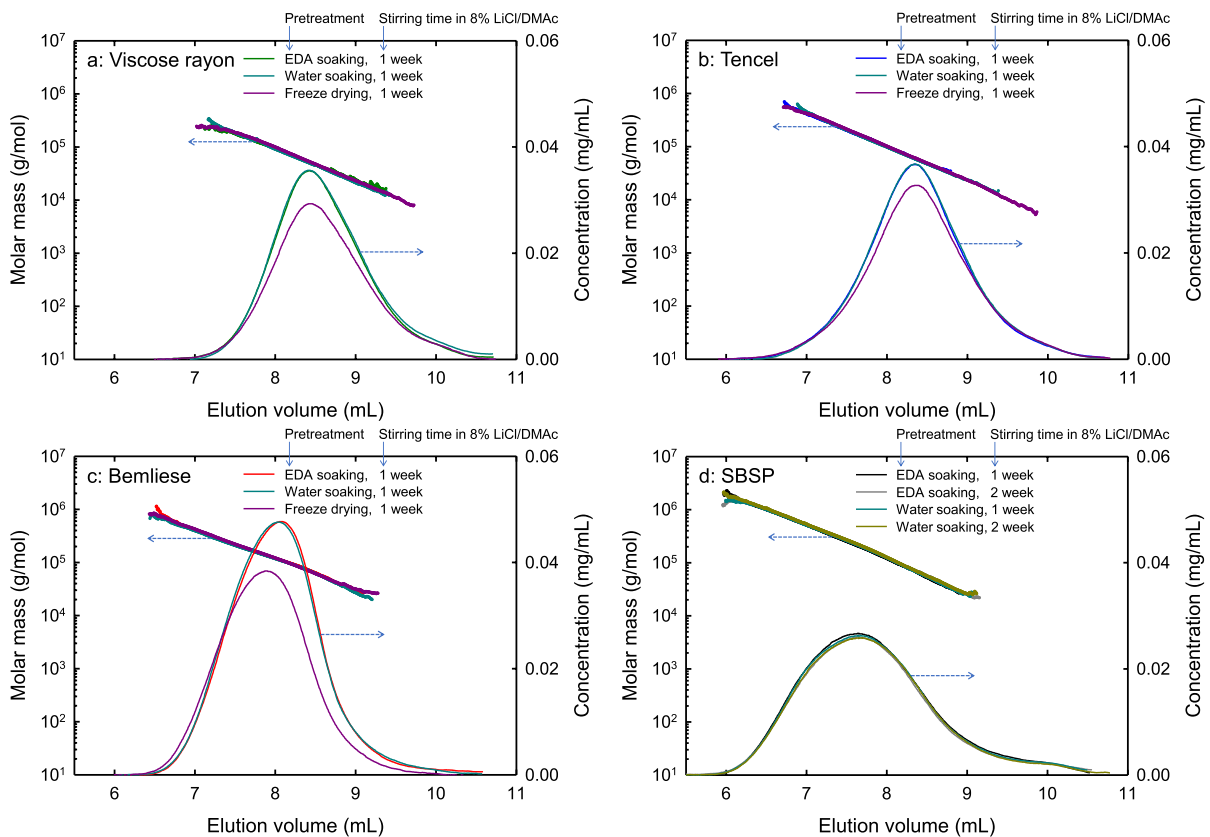


Fig. 3 Molar mass plots and SEC-elution patterns of **a** viscose rayon, **b** Tencel, **c** Bemliese, and **d** SBSP dissolved in 8% (w/w) LiCl/DMAc following the three activation methods and stirring for 1 week before dilution to 1% (w/v) LiCl/DMAc

pretreated viscose rayon samples. Furthermore, no significant differences in the molar mass plots and SEC-elution patterns were observed between the viscose rayon samples stirred in 8% (w/w) LiCl/DMAc for 1 and 2 weeks, showing that stirring the pretreated viscose rayon sample in 8% (w/w) LiCl/DMAc for 1 week is sufficient to obtain constant SEC/MALLS data.

The SEC/MALLS results of Tencel are shown in Fig. 3b, Figs. S5–S7, and Tables S4–S6. The molar mass plots for the three pretreatments agreed well, and the peak area of the SEC-elution pattern of freeze-dried Tencel was smaller than those of Tencel pretreated by the other two methods (Fig. 3b). However, the molar mass parameters of the Tencel samples, except for the calculated mass values (Tables S4–S6), were similar for the samples pretreated by the three methods. No significant differences in the molar mass plots or SEC-elution patterns were observed for the Tencel samples stirred in 8% (w/w) LiCl/DMAc for different times. Stirring the pretreated Tencel sample in 8% (w/w) LiCl/DMAc for 1 week was sufficient to obtain constant SEC/MALLS analysis data.

The SEC/MALLS results of Bemliese are shown in Fig. 3c, Figs. S8–S10, and Tables S7–S9. The molar mass plot was the same line regardless of the pretreatment (Fig. 3c). The SEC-elution patterns of Bemliese pretreated by EDA and water soaking were similar. However, the peak area and SEC-elution pattern for the freeze-dried Bemliese sample were different from those pretreated by EDA and water soaking. Not only the calculated mass values, but also the other molar mass parameters of the freeze-dried Bemliese were different from those of the EDA- and water-pretreated samples (Tables S7–S9). The M_n , M_w , and DP_w values of freeze-dried Bemliese were higher than those of EDA- and water-pretreated Bemliese, whereas the calculated mass values were lower. Thus, the SEC/MALLS data obtained for the EDA- and water-pretreated samples were regarded as being constant and more accurate than those of the freeze-dried sample.

The SEC/MALLS data of SBSP are shown in Fig. 3d and Table S10. The molar mass plot was the same regardless of the pretreatment and stirring time, and the SEC-elution patterns were almost the same (Fig. 3d). All of the molar mass parameters were similar for the samples pretreated by the two methods (Table S10).

Discussion

As described in the previous section, the molar mass parameters, including the calculated mass values, of EDA- and water-pretreated viscose rayon, Tencel, Bemliese, and SBSP were similar. Consequently, EDA pretreatment resulted in almost no mass loss of the low-molar-mass fractions in the three regenerated cellulose samples and SBSP used in this study. Furthermore, the SEC/MALLS data for the cellulose samples obtained after stirring the EDA- and water-pretreated samples in 8% (w/w) LiCl/DMAc for 1 week can be regarded as being reproducible and constant for analytical studies of their molar masses and molar mass distributions.

The representative molar mass plots and SEC-elution patterns of the three regenerated cellulose samples and SBSP pretreated by EDA soaking are shown in Fig. 4a, in which the peak-top heights of the SEC-elution patterns were adjusted to be similar. All of

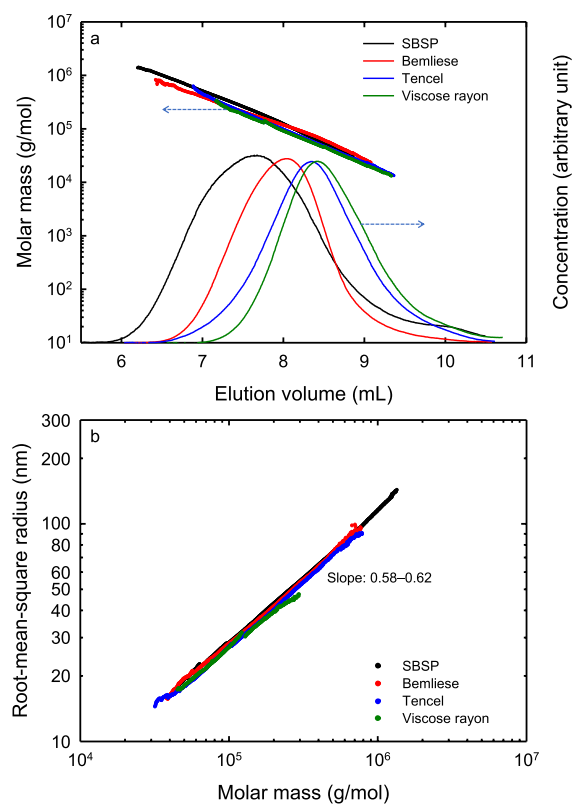


Fig. 4 **a** Molar mass plots and SEC-elution patterns of the three regenerated cellulose samples and SBSP and **b** the corresponding double logarithmic plots (or conformation plots)

the SEC-elution patterns showed mostly single peaks without additional low-molar-mass peaks owing to, for instance, hemicelluloses (Ono et al. 2020, 2022a, b). The hemicellulose molecules originally present in the softwood chips were mostly removed by the acid sulfite pulping and subsequent bleaching processes for production of SBSP, differing from softwood and hardwood bleached kraft pulps (Ono et al. 2017, 2018). The peak-top elution volume increased in the order of SBSP < Bemliese < Tencel < viscose rayon, showing that their molar masses decreased in the opposite order of SBSP > Bemliese > Tencel > viscose rayon. All of the molar mass plots were roughly on the same line and the molar mass decreased with increasing SEC-elution volume. This showed that all of the cellulose molecules in the four samples were dispersed in 1% (w/v) LiCl/DMAc at the individual molecular level without forming any aggregates, and they were suitably separated by the SEC column depending on their sizes.

Double logarithmic plots, or conformation plots, of the four cellulose samples shown in Fig. 4a are shown in Fig. 4b. All of the plots were roughly on the same line, and the slopes were 0.58–0.62, showing that all of the cellulose molecules in the four samples had linear random-coil conformations in 1% (w/v) LiCl/DMAc without any branched or shrunk structures. This is reasonable as pure β -(1→4)-linked glucans. We have reported that softwood holocellulose samples, softwood bleached kraft pulps (SBKPs), 17.5% NaOH-extracted softwood holocellulose and SBKP samples (i.e., α -cellulose samples prepared from softwood holocellulose and SBKP samples, respectively), and dilute acid-hydrolyzed SBKP show conformation plots with slope values of < 0.45. These results

indicate that some cellulose molecules in the high-molar-mass fractions of these samples have branched structures with glucomannan through lignin molecules or lignin fragments (Ono et al. 2017, 2018; Ono and Isogai 2020). Differing from the above softwood-originating samples, SBSP did not have branched structures as in the cases of hardwood kraft pulps and cotton, bacterial, tunicate, and algal cellulose samples (Ono et al. 2016b, 2017, 2018). This is the reason why SBSP is used as dissolving pulp fibers for production of regenerated cellulose samples and cellulose derivatives.

The molar mass parameters of the four cellulose samples are summarized in Table 1. The average values for the viscose rayon and Tencel samples were calculated from those obtained for the EDA-pretreated, water-pretreated, and freeze-dried samples. For Bemliese, the average values were calculated from those of only the EDA- and water-pretreated samples. The values obtained for freeze-dried Bemliese were excluded because they were clearly different from those obtained for the EDA- and water-pretreated samples, as described in the previous section (Tables S7–S9 in the Electronic Supplementary Material).

When the Mark–Houwink–Sakurada equation, $[\eta] = 0.909 \times DP_v^{0.9}$, was used, the average DP_v value was similar to that of the average DP_w value for each regenerated cellulose sample. However, the average DP_v value of SBSP (610) was much lower than the DP_w value (1810) determined by SEC/MALLS. The DP_v values of SBSP were almost unchanged for the SBSP/Cu(EDA)₂(OH)₂ solutions stirred for 10, 20, and 40 min. This clear discrepancy between the DP_v and DP_w values for SBSP may have been

Table 1 Molar mass parameters of the regenerated cellulose samples and SBSP determined by SEC/MALLS and viscosity methods

Sample	SEC/MALLS						DP_v
	M_n	M_w	DP_w^a	M_w/M_n	Calculated mass (μ g)	Slope of conformation plots	
Viscose rayon	26,900 ± 1600	54,400 ± 1500	340 ± 10	2.0 ± 0.1	48 ± 1	0.58	330 ± 3
Tencel	32,700 ± 1100	86,600 ± 3300	530 ± 20	2.0 ± 0.2	51 ± 4	0.59	400 ± 2
Bemliese ^b	87,600 ± 4400	143,100 ± 1160	880 ± 7	1.6 ± 0.1	65 ± 2	0.59	800 ± 3
SBSP	72,200 ± 1800	293,100 ± 9200	1810 ± 60	4.1 ± 0.2	52 ± 1	0.62	610 ± 1

^a $DP_w = M_w/162$

^bThe average SEC/MALLS data were obtained from the data for the EDA- and water-activated samples, excluding those for the freeze-dried samples

caused by the stability of SBSP in the alkaline 0.5 M $\text{Cu}(\text{EDA})_2(\text{OH})_2$ solution. The SBSP sample may have contained some chemical structures susceptible to depolymerization by the alkaline $\text{Cu}(\text{EDA})_2(\text{OH})_2$ solution. Generally, the C=O groups in cellulosic pulps cause depolymerization by β -alkoxy elimination under alkaline conditions, although the presence of such C=O groups could not be detected in the solid-state ^{13}C -NMR spectrum of SBSP (Figs. 2 and S1). Thus, a small amount of C=O groups present randomly along each cellulose molecule of SBSP may have caused the low DP_v value.

Although the solid-state ^{13}C -NMR spectra of the regenerated cellulose samples indicated the presence of C=O groups as small peaks at ~ 97 ppm (Fig. 2), there were no significant differences between the DP_w and DP_v values (Table 1). This is probably because the C=O groups susceptible to the alkaline $\text{Cu}(\text{EDA})_2(\text{OH})_2$ solution are located close to both ends of each cellulose chain in the regenerated cellulose samples, whereas the C=O groups in SBSP are located more randomly along each cellulose chain. However, this is speculative, and further studies are needed to clarify the reason for the discrepancy between the DP_v and DP_w values for SBSP.

Conclusions

The three commercial regenerated cellulose samples, viscose rayon, Tencel, and Bemliese, exhibited similar solid-state ^{13}C -NMR spectra to low-crystallinity cellulose II. The ^{13}C -NMR spectra of the three samples had small peaks at ~ 97 ppm, which may be ascribed to the hydrated C6-aldehyde groups formed during the commercial fiber production processes. The three regenerated cellulose samples were dissolved in 8% (w/w) LiCl/DMAc by EDA-soaking, water-soaking, and freeze-drying pretreatment and subsequent stirring of the pretreated samples in 8% (w/w) LiCl/DMAc for 1 week. Based on the calculated mass values obtained by SEC/MALLS, almost all of the cellulose molecules in the EDA- and water-pretreated regenerated cellulose samples were dissolved in 8% (w/w) LiCl/DMAc and subjected to SEC/MALLS without significant mass loss. However, 10%–20% of the freeze-dried samples were not subjected to SEC/MALLS, probably because of incomplete dissolution in 8% (w/w) LiCl/DMAc. The average M_n and M_w

values calculated from the SEC/MALLS data were almost the same as those obtained for the EDA- and water-pretreated samples. The average DP_w values were calculated to be 340, 530, 880, and 1810 for viscose rayon, Tencel, Bemliese, and SBSP, respectively. The conformation plots of the samples had slopes of 0.58–0.62, showing that all of the cellulose molecules in the four samples were dissolved in 1% (w/v) LiCl/DMAc, forming linear random-coil conformations. For the regenerated cellulose samples, the DP_w values determined by SEC/MALLS were similar to the corresponding DP_v values. However, for SBSP, the DP_v values were lower than the DP_w values, indicating the inaccuracy of the DP_v values of SBSP.

Acknowledgments We thank Edanz for editing a draft of this manuscript.

Authors contributions All of the authors contributed to conception, design, the experiments, and the analyses. All of the authors read and approved the final manuscript. The manuscript was approved by all of the authors for publication.

Funding Open access funding provided by The University of Tokyo. This study was supported in part by the New Energy and Industrial Technology Development Organization (NEDO), Japan.

Declarations

Competing interests The authors declare no competing interests.

Conflict of interest The authors declare that they have no known competing financial interests or personal relationships that could have appeared to influence this study.

Ethical approval and consent to participate This article does not contain any studies with human participants or animals performed by any of the authors.

Open Access This article is licensed under a Creative Commons Attribution 4.0 International License, which permits use, sharing, adaptation, distribution and reproduction in any medium or format, as long as you give appropriate credit to the original author(s) and the source, provide a link to the Creative Commons licence, and indicate if changes were made. The images or other third party material in this article are included in the article's Creative Commons licence, unless indicated otherwise in a credit line to the material. If material is not included in the article's Creative Commons licence and your intended use is not permitted by statutory regulation or exceeds the permitted use, you will need to obtain permission directly from the copyright holder. To view a copy of this licence, visit <http://creativecommons.org/licenses/by/4.0/>.

References

- Abu-Rous M, Varga K, Bechtold T, Schuster KC (2007) A new method to visualize and characterize the pore structure of TENCEL (Lyocell) and other man-made cellulosic fibres using a fluorescent dye molecular probe. *J Appl Polym Sci* 106:208–32091. <https://doi.org/10.1002/app.26722>
- Ago M, Endo T, Hirotsu T (2004) Crystalline transformation of native cellulose from cellulose I to cellulose II polymorph by a ball-milling method with a specific amount of water. *Cellulose* 11:163–167. <https://doi.org/10.1023/B:CELL.0000025423.32330.fa>
- Bikova T, Treimanis A (2002) Problems of the MMD analysis of cellulose by SEC using DMA/LiCl: a review. *Carbohydr Polym* 48:23–28. [https://doi.org/10.1016/S0144-8617\(01\)00207-7](https://doi.org/10.1016/S0144-8617(01)00207-7)
- Biliuta G, Fras L, Strnad S, Harabagiu V, Coseri S (2010) Oxidation of cellulose fibers mediated by nonpersistent nitroxyl radicals. *J Polym Sci Part a: Polym Chem* 48:4790–4799. <https://doi.org/10.1002/pola.24270>
- Borbély E (2008) Lyocell, the new generation of regenerated cellulose. *Acta Polytech Hungarica* 5:11–18
- Cao X, Ding B, Yu J, Al-Deyab SS (2012) Cellulose nanowhiskers extracted from TEMPO-oxidized jute fibers. *Carbohydr Polym* 90:1075–1080. <https://doi.org/10.1016/j.carbpol.2012.06.046>
- Duchemin BJCZ, Newman RH, Staiger MP (2007) Phase transformations in microcrystalline cellulose due to partial dissolution. *Cellulose* 14:311–320. <https://doi.org/10.1007/s10570-007-9121-4>
- Dudley RL, Fyfe CA, Stephenoson PJ, Deslandes Y, Hamer GK, Marchessault RH (1983) High-resolution carbon-13 CP/MAS NMR spectra of solid cellulose oligomers and the structure of cellulose II. *J Am Chem Soc* 105:2469–2472. <https://doi.org/10.1021/ja00346a059>
- Dupont AL (2003) Cellulose in lithium chloride/N,N-dimethylacetamide, optimization of a dissolution method using paper substrates and stability of the solutions. *Polymer* 44:4117–4126. [https://doi.org/10.1016/S0032-3861\(03\)00398-7](https://doi.org/10.1016/S0032-3861(03)00398-7)
- Fadavi F, Abdulkhani A, Zadeh ZE, Hamzeh Y (2021) Influence of swelling media on the crystallinity and accessibility of lyocell fibers: An FTIR and ¹³C NMR analysis. *J Nat Fiber* 19:6365–6376. <https://doi.org/10.1080/15440478.2021.1916675>
- Fink HP, Weigle P, Ganster J (2001) Structure formation of regenerated cellulose materials from NMMO-solutions. *Prog Polym Sci* 26:1473–1524. [https://doi.org/10.1016/S0079-6700\(01\)00025-9](https://doi.org/10.1016/S0079-6700(01)00025-9)
- Follain N, Marais MF, Montanari S, Vignon MR (2010) Coupling onto surface carboxylated cellulose nanocrystals. *Polmer* 51:5332–5344. <https://doi.org/10.1016/j.polym.2010.09.001>
- From M, Larsson PT, Andreasson B, Medroho B, Svanedal I, Edlund H, Norgren M (2020) Tuning the properties of regenerated cellulose: effects of polarity and water solubility of the coagulation medium. *Carbohydr Polym* 236:116068. <https://doi.org/10.1016/j.carbpol.2020.116068>
- Funahashi R, Okita Y, Hondo H, Zhao M, Saito T, Isogai A (2017) Different conformations of surface cellulose molecules in native cellulose microfibrils revealed by layer-by-layer peeling. *Biomacromolecules* 18:3687–3694. <https://doi.org/10.1021/acs.biomac.7b01173>
- Henniges U, Vejdovszky P, Siller M, Jeong MJ, Rosenau T, Potthast A (2014) Finally dissolved! Activation procedures to dissolve cellulose in DMAc/LiCl prior to size exclusion chromatography analysis – A review. *Curr Chromatogr* 1:52–68. <https://doi.org/10.2174/2213240601666131118220030>
- Horii F, Hirai A, Kitamaru R (1982) Solid-state high-resolution ¹³C-NMR studies of regenerated cellulose samples with different crystallinities. *Polym Bull* 8:163–170. <https://doi.org/10.1007/BF00263023>
- Horii F, Hirai A, Kitamaru R (1983) Solid-state ¹³C-NMR study of conformations of oligosaccharides and cellulose - conformation of CH₂OH group about the exo-cyclic C-C bond. *Polym Bull* 10:357–361. <https://doi.org/10.1007/BF00281948>
- Ibbett RN, Domvoglou D, Fasching M (2007) Characterisation of the supramolecular structure of chemically and physically modified regenerated cellulosic fibres by means of high-resolution Carbon-13 solid-state NMR. *Polymer* 48:1287–1269. <https://doi.org/10.1016/j.polymer.2006.12.034>
- Idström A, Schantz S, Sundberg J, Chmelka BF, Gatenholm P, Nordstierna L (2016) ¹³C NMR assignments of regenerated cellulose from solid-state 2D NMR spectroscopy. *Carbohydr Polym* 151:480–487. <https://doi.org/10.1016/j.carbpol.2016.05.107>
- Isogai A, Usuda M, Kato T, Uryu T, Atalla RH (1989a) Solid-state CP/MAS ¹³C NMR study of cellulose polymorphs. *Macromolecules* 22:3168–3172. <https://doi.org/10.1021/ma00197a045>
- Isogai A, Mutoh N, Onabe F, Usuda M (1989b) Viscosity measurements of cellulose/SO₂-amine-dimethylsulfoxide solution. *Sen'i Gakkaishi* 45:299–306. https://doi.org/10.2115/fiber.45.7_299
- Isogai A, Saito T, Fukuzumi H (2011) TEMPO-oxidized cellulose nanofibers. *Nanoscale* 3:71–85. <https://doi.org/10.1039/c0nr00583e>
- Isogai A, Hänninen T, Fujisawa S, Saito T (2018) Catalytic oxidation of cellulose with nitroxyl radicals under aqueous conditions. *Prog Polym Sci* 86:122–148. <https://doi.org/10.1016/j.progpolymsci.2018.07.007>
- Isogai A (2022) TEMPO-catalyzed oxidation of polysaccharides. *Polym J* 54:387–402. <https://doi.org/10.1038/s41428-021-00580-1>
- Jin H, Zha C, Gu L (2007) Direct dissolution of cellulose in NaOH/thiourea/urea aqueous solution. *Carbohydr Res* 342:851–858. <https://doi.org/10.1016/j.carres.2006.12.023>
- Kreze T, Malej S (2003) Structural characteristics of new and conventional regenerated cellulose fibers. *Text Res J* 73:675–684. <https://doi.org/10.1177/0040517503073008>
- Kuchtoá G, Herink P, Herink T, Chýlková J, Mikulášek P, Dušek L (2023) From lab-scale to pilot-scale treatment of real wastewater from the production of rayon fiber. *Process Saf Environ* 171:834–846. <https://doi.org/10.1016/j.psep.2023.01.059>

- Larsson PT, Westlund PO (2005) Line shapes in CP/MAS ^{13}C NMR spectra of cellulose I. *Spectrochim Acta Part A* 62:539–546. <https://doi.org/10.1016/j.saa.2005.01.021>
- Li R, Zhang L, Xu M (2012) Novel regenerated cellulose films prepared by coagulating with water: structure and properties. *Carbohydr Polym* 87:95–100. <https://doi.org/10.1016/j.carbpol.2011.07.023>
- Li Z, Sathitsuksanoh N, Zhang W, Goodell B, Rennecker S (2017) Towards an understanding of cellulose microfibril dimensions from TEMPO-oxidized pulp fiber. *ACS Symp Ser* 1251:55–73. <https://doi.org/10.1021/bk-2017-1251.ch003>
- Li H, Legere S, He Z, Zhang H, Li J, Yang B, Zhang S, Zhang L, Zheng L, Ni Y (2018) Methods to increase the reactivity of dissolving pulp in the viscose rayon production process: a review. *Cellulose* 25:3733–3753. <https://doi.org/10.1007/s10570-018-1840-1>
- Lin F, You Y, Yang X, Jiang X, Lu Q, Wang T, Huang B, Lu B (2017) Microwave-assisted facile synthesis of TEMPO-oxidized cellulose beads with high adsorption capacity for organic dyes. *Cellulose* 24:5025–5040. <https://doi.org/10.1007/s10570-017-1473-9>
- Marx M (1955) Viskosimetrische molekulargewichtsbestimmung von cellulose in kupfer-äthylendiamin. *Makromol Chem* 14:157–176. <https://doi.org/10.1002/macp.1955.020160118>
- Maunu S, Liitiä T, Kauliomäki S, Hortling B, Sundquist J (2000) ^{13}C CP/MAS NMR investigations of cellulose polymorphs in different pulps. *Cellulose* 7:147–159. <https://doi.org/10.1023/A:1009200609482>
- Mendes ISF, Prates A, Evtuguin DV (2021) Production of rayon fibres from cellulosic pulps: state of the art and current developments. *Carbohydr Polym* 273:118466. <https://doi.org/10.1016/j.carbpol.2021.118466>
- Mori T, Chikayama E, Tsuboi Y, Ishida N, Shisa N, Noritake Y, Moriya S, Kikuchi J (2012) Exploring the conformational space of amorphous cellulose using NMR chemical shifts. *Carbohydr Polym* 90:1197–1203. <https://doi.org/10.1016/j.carbpol.2012.06.027>
- Moulthrop JS, Swatloski RP, Moyna G, Rogers RD (2005) High-resolution ^{13}C NMR studies of cellulose and cellulose oligomers in ionic liquid solutions. *Chem Commun* 2005:1557–1559. <https://doi.org/10.1039/B417745B>
- Newman RH, Hemmingson J (1994) Carbon-13 NMR distinction between categories of molecular order and disorder in cellulose. *Cellulose* 2:95–110. <https://doi.org/10.1007/BF00816383>
- Nomura S, Kugo Y, Erata T (2020) ^{13}C NMR and XRD studies on the enhancement of cellulose II crystallinity with low concentration NaOH posttreatments. *Cellulose* 27:3553–3563. <https://doi.org/10.1007/s10570-020-03036-6>
- Ono Y, Ishida T, Soeta H, Saito T, Isogai A (2016a) Reliable dn/dc values of cellulose, chitin, and cellulose triacetate dissolved in LiCl/N, N-dimethylacetamide for molecular mass analysis. *Biomacromol* 17:192–199. <https://doi.org/10.1021/acs.biomac.5b01302>
- Ono Y, Tanaka R, Funahashi R, Takeuchi M, Saito T, Isogai A (2016b) SEC–MALLS analysis of ethylenediamine-pretreated native celluloses in LiCl/N, N-dimethylacetamide: softwood kraft pulp and highly crystalline bacterial, tunicate, and algal celluloses. *Cellulose* 23:1639–1647. <https://doi.org/10.1007/s10570-016-0948-4>
- Ono Y, Saito T, Isogai A (2017) Branched structures of softwood celluloses: proof based on size-exclusion chromatography and multi-angle laser-light scattering. *Nanocellul. Prep. Prop Appl.* 1251:151–169. <https://doi.org/10.1021/bk-2017-1251.ch008>
- Ono Y, Funahashi R, Saito T, Isogai A (2018) Investigation of stability of branched structures in softwood cellulose using SEC/MALLS/RI/UV and sugar composition analysis. *Cellulose* 25:2667–2679. <https://doi.org/10.1007/s10570-018-1713-7>
- Ono Y, Isogai A (2020) Analysis of celluloses, plant hemicelluloses, and wood pulps by size-exclusion chromatography/multi-angle laser-light scattering. *Carbohydr Polym* 251:117045. <https://doi.org/10.1016/j.carbpol.2020.117045>
- Ono Y, Takeuchi M, Isogai A (2021) TEMPO/NaBr/NaClO and NaBr/NaClO oxidations of cotton linters and ramie celluloses. *Cellulose* 28:6035–6049. <https://doi.org/10.1007/s10570-021-03944-1>
- Ono Y, Takeuchi M, Isogai A (2022a) Changes in neutral sugar composition, molar mass and molar mass distribution, and solid-state structures of birch and Douglas fir by repeated sodium chlorite delignification. *Cellulose* 29:2119–2129. <https://doi.org/10.1007/s10570-022-04448-2>
- Ono Y, Takeuchi M, Zhou Y, Isogai A (2022b) Characterization of cellulose and TEMPO-oxidized celluloses prepared from Eucalyptus globulus. *Holzforschung* 76:169178
- Ono Y, Takeuchi M, Kimura S, Puangsin B, Wu CN, Isogai A (2022c) Structures, molar mass distributions, and morphologies of TEMPO-oxidized bacterial cellulose fibrils. *Cellulose* 29:4977–4992. <https://doi.org/10.1007/s10570-022-04617-3>
- Östlund Å, Idström A, Olsson C, Larsson PT, Nordstierna L (2013) Modification of crystallinity and pore size distribution in coagulated cellulose films. *Cellulose* 20:1657–1667. <https://doi.org/10.1007/s10570-013-9982-7>
- Potthast A, Röhring J, Rosenau T, Borgards A, Sixta H, Kosma P (2003) A novel method for the determination of carbonyl groups in celluloses by fluorescence labeling. 3. Monitoring oxidative processes. *Biomacromolecules* 4:743–749. <https://doi.org/10.1021/bm025759c>
- Sayyed AJ, Deshmukh NA, Pinjari DV (2019) A critical review of manufacturing processes used in regenerated cellulose fibres: viscose, cellulose acetate, cuprammonium, LiCl/DMAc, ionic liquids, and NMMO based lyocell. *Cellulose* 26:2913–2940. <https://doi.org/10.1007/s10570-019-02318-y>
- Schulz GV, Dinglinger A (1941) Molekulargewichtsbestimmungen an einer Reihe von Polymethacrylsäuremethylestern nach verschiedenen Methoden [osmotisch, viscosimetrisch und durch Fällungstitration]. *J Prakt Chem* 158:136–162. <https://doi.org/10.1002/prac.19411580113>
- Shanshan G, Jianqin W, Zhengwei J (2012) Preparation of cellulose films from solution of bacterial cellulose in NMMO. *Carbohydr Polym* 87:1020–1025. <https://doi.org/10.1016/j.carbpol.2011.06.040>
- Shinoda R, Saito T, Okita Y, Isogai A (2012) Relationship between length and degree of polymerization of

- TEMPO-oxidized cellulose nanofibrils. *Biomacromol* 13:842–849. <https://doi.org/10.1021/bm2017542>
- Silbermann S, Weilach C, Kliba G, Fackler K, Potthast A (2017) Improving molar mass analysis of cellulose samples with limited solubility. *Carbohydr Polym* 178:302–310. <https://doi.org/10.1016/j.carbpol.2017.09.031>
- Siller M, Ahn K, Pircher N, Rosenau T, Potthast A (2014) Dissolution of rayon fibers for size exclusion chromatography: a challenge. *Cellulose* 21:3291–3301. <https://doi.org/10.1007/s10570-014-0356-6>
- Veit D (2022) Cellulosic man-made fibers. In: *Fibers: history, production, properties, market*. Springer Nature Switzerland, Switzerland, pp. 1831–882. <https://doi.org/10.1007/978-3-031-15309-9>
- Wei X, Wang Y, Li J, Wang F, Chang G, Fu T, Zhou W (2018) Effects of temperature on cellulose hydrogen bonds during dissolution in ionic liquid. *Carbohydr Polym* 201:387–391. <https://doi.org/10.1016/j.carbpol.2018.08.031>
- Yamamoto M, Kuramae R, Yanagisawa M, Ishii D, Isogai A (2011) Light-scattering analysis of native wood holocelluloses totally dissolved in LiCl-DMI solutions: high probability of branched structures in inherent cellulose. *Biomacromolecules* 12:3982–3988. <https://doi.org/10.1021/bm201211z>
- Yang H, Wang T, Oehme D, Petridis L, Hong M, Kubicki JD (2018) Structural factors affecting ^{13}C NMR chemical shifts of cellulose: a computational study. *Cellulose* 25:23–36. <https://doi.org/10.1007/s10570-017-1549-6>
- Yuan S, Tyufekchiev MV, Timko MT, Schmidt-Rohr K (2022) Direct quantification of the degree of polymerization of hydrolyzed cellulose by solid-state NMR spectroscopy. *Cellulose* 29:2131–3144. <https://doi.org/10.1007/s10570-022-04433-9>
- Zhang X, Xiao N, Wang H, Liu C, Pan X (2018) Preparation and characterization of regenerated cellulose film from a solution in lithium bromide molten salt hydrate. *Polymers* 10:614. <https://doi.org/10.3390/polym10060614>
- Zhao H, Kwak JH, Wang Y, Franz JA, White JM, Holladay JE (2007) Interactions between cellulose and *N*-methylmorpholine-*N*-oxide. *Carbohydr Polym* 67:97–103. <https://doi.org/10.1016/j.carbpol.2006.04.019>
- Zhou Y, Ono Y, Takeuchi M, Isogai A (2020) Changes to the contour length, molecular chain length, and solid-state structures of nanocellulose resulting from sonication in water. *Biomacromolecules* 21:2346–2355. <https://doi.org/10.1021/acs.biomac.0c00281>

Publisher's Note Springer Nature remains neutral with regard to jurisdictional claims in published maps and institutional affiliations.